*Pesquisas em Geociências*, 41 (3): 273-285, set./dez. 2014 ISSN 1518-2398
Instituto de Geociências, Universidade Federal do Rio Grande do Sul, Porto Alegre, RS, Brasil E-ISSN 1807-9806

# Numerical analyses of wave propagation over the inner shelf and shoreface of the southern Brazilian coast: from Torres to Mostardas

Jair Vignolle da SILVA[1], Paulo Roberto de Freitas TEIXEIRA[2] & Lauro Júlio CALLIARI[3]

1. CINAT/Matemática, Instituto Federal de Educação, Ciência e Tecnologia. Praça Vinte de Setembro, 455, CEP 96015-360, Centro, Pelotas, RS, Brasil. E-mail: jairvig@ig.com.br.
2. Escola de Engenharia, Universidade Federal do Rio Grande. Avenida Itália, km 8, CEP 96202-900, Campus Carreiros, Rio Grande, RS, Brasil. E-mail: pauloteixeira@furg.br.
3. Instituto de Oceanografia, Universidade Federal do Rio Grande. Avenida Itália, km 8, CEP 96202-900, Campus Carreiros, Rio Grande, RS, Brasil. E-mail: lcalliari@log.furg.br.

Recebido em 12/2013. Aceito para publicação em 11/2014.
Versão online publicada em 04/12/2014 (*www.pesquisasemgeociencias.ufrgs.br*)

**Abstract -** The shoreface and the inner shelf along the northern and the central coast of Rio Grande do Sul (RS) state, Brazil, between Torres and Mostardas, although displaying a homogeneous bottom relief show variations in slope and width. In the northern sector, between Torres and Pinhal, the inner shelf is wide, while the shoreface is narrow. Towards the south, these patterns are just the opposite. In this study, a model based on the parabolic approximation of the mild slope equation, REF/DIF 1, is used to simulate the wave propagation in this region. Wave refraction diagrams based on the predominant wave climate show a dominant and invariable divergent pattern for wave incidence from 90° to 135°. Numerical analyses of changes in wave energy, regarding differences in width and slope using a bottom friction coefficient *fw* = 0.01 in the different coastal sectors, show little influence of the bottom friction over the wave transformation processes. In general, a friction coefficient *fw* = 0.2 shows that wave energy reduction due to bottom friction over the wider shoreface south of Pinhal by comparison with the sector to the north is compensated by its shorter inner shelf width. The analyses show that lateral gradients of wave energy along the 10 m isobaths regarding the morphological differences between the two sectors are negligible.
**Keywords:** wave transformation, shoreface, refraction, diffraction, numerical simulation.

**Resumo -** Análise numérica da propagação de ondas sobre a plataforma continental interna e antepraia da costa sul do Brasil: de Torres a Mostardas. A plataforma continental interna e a antepraia ao longo do litoral norte e médio do estado do Rio Grande do Sul (RS), Brasil, entre Torres e Mostardas, têm o relevo do fundo homogêneo, mas apresentam variações de inclinação e largura. No setor norte, entre Torres e Pinhal, a plataforma interna é mais larga, enquanto a largura de antepraia é mais estreita. Por outro lado, o oposto ocorre ao Sul de Pinhal. Este trabalho analisa numericamente a propagação de ondas nesta região através do REF/DIF 1, modelo que adota a aproximação parabólica da equação de declive suave. Os diagramas de refração de ondas, baseados em um clima de onda predominante, indicam que o padrão dominante é o divergente para ondas incidentes de 90° a 135°. Análises numéricas das variações de energia de ondas, investigando a influência das variações da largura da plataforma interna e da largura de antepraia, e da fricção com o fundo considerando um coeficiente de atrito *fw* = 0,01, revelam a pouca influência do atrito com o fundo sobre a transformação das ondas. Adotando-se um coeficiente de atrito *fw* = 0,2, constata-se, de forma geral, que a influência do aumento da largura da antepraia do sul de Pinhal para o norte no atrito com o fundo é compensada pela influência da diminuição da largura da plataforma continental interna. As análises mostram que os gradientes laterais da energia da onda ao longo da isobatimétrica de 10 m, mesmo considerando as diferenças morfológicas entre os dois setores, são desprezíveis.
**Palavras-chave:** transformação de ondas, antepraia, refração, difração, simulação numérica.

## 1 Introduction

Information about wave characteristics is essential for studies of coastal and ocean engineering problems. Usually, wave height and direction in the coastal region are determined by the knowledge of the deep water wave characteristics. Increased demand to accurately investigate wave design conditions, sediment transport and surf-zone currents has significantly improved numerical models to forecast wave transformation processes in the last decades (Liu & Losada, 2002).

As the waves approach the coast, changes in bathymetry and bottom types, besides artificial structures, can affect wave direction and velocity, energy dissipation and redistribution. Furthermore, inside the breaking zone, waves undergo several important and complex transformations (Liu, 1990).

The northern sector of the Rio Grande do Sul (RS)

coast, in Brazil, between Torres and Mostardas (Fig. 1), displays a wide continental shelf (130 km on average) and the isobaths run parallel to the coastline orientation (NE-SW). Although the inner shelf and the shoreface are relatively smooth, there is a marked difference in the widths of these two bathymetric provinces to the north and the south of Pinhal (Fig. 1). The shoreface limited by the 20 m isobath between Mostardas and Pinhal is wider (9 km) than that corresponding to the sector between Pinhal and Torres (5.9 km). Moreover, the limit of the inner shelf defined by the 50 m isobath presents an inverse pattern of that displayed by the shoreface, being wider in the sector Torres-Pinhal (44 km) than in the sector Pinhal-Mostardas (24 km). Although being relatively straight, the RS coast displays several alongshore undulations. Pinhal can be considered an inflexion point separating a protuberance from an embayment. The protuberance is represented by a linear shoal "Banco da Berta" which is 30 km long and defined by the eastward inflexion of the 14 m isobath.

Since the shoreface plays an important role in wave energy dissipation (Wright *et al*., 1987), we aim at addressing the effect of variable shoreface and inner shelf widths on the waves propagating shoreward. Thus, the general objective of this paper is to analyze changes in wave energy varying the angle of incidence, period and wave height in these distinct sectors between Torres and Mostardas. Taking into account changes in bathymetry and bottom friction coefficients of the shoreface and the inner shelf, the importance of bottom friction in wave propagation is investigated. What roles do the morphologically different shoreface regions fronting the beaches play in the wave transformation processes regarding wave height ? Is there any gradient in wave energy along the coast ? Unlike the zones analyzed by Wright *et al*. (1987) along the Virginia coast in the US (where the widths of the inner shelf are similar and the ones of the shoreface vary between sectors), in the RS coast, the widths of both sectors are different. There may be compensation in terms of wave energy dissipation due to bottom friction.

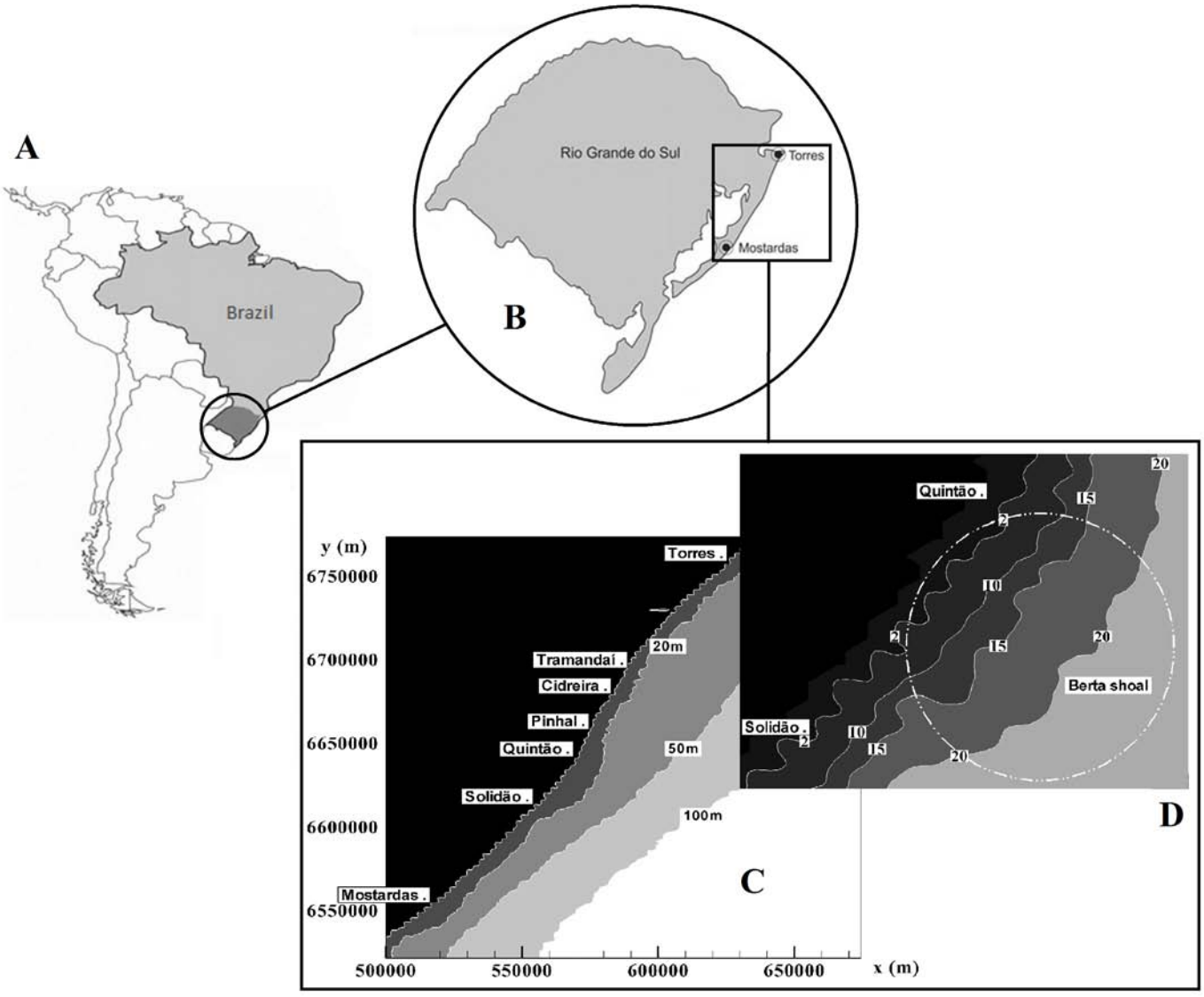


Figure 1. Location of the study region (A and B); coastal configuration and bathymetry of the shoreface and the inner shelf in the area between Torres and Mostardas (C); and detail (D) of the Berta shoal (Mercator Projection – MC 51°).

Due to poor information about the wave climate along the RS coast, numerical modeling is an important way to characterize the main processes of wave propagation from deep water to the coast. Some authors of earlier studies in this area (Pimenta, 1999; Speranski & Calliari, 2006) used simplified models based on refraction and shoaling applied to a regional scale (hundreds of km). Neither bottom friction nor diffraction was contemplated. The numerical model used in this simulation, based on the parabolic approximation of the mild slope equation, REF/DIF 1 (Kirby & Dalrymple, 1994), takes into account all wave transformation processes from deep to shallow waters. Wright *et al.* (1987) investigated the beach dynamics on the Virginia state coast, between *Cape Henry* and *False Cape*, by using the RCPWAVE code (Ebersole, 1985). Considering the bottom topography and morphology, the authors concluded that most wave energy dissipation due to the friction occurs in the nearshore.

## 2 Materials and methods

REF/DIF 1 (Kirby & Dalrymple, 1994) is a wave propagation and deformation model applied to areas of variable depth based on the parabolic approximation of the mild slope equation using the Minimax method (Kirby, 1986). In this equation, there is a dissipation factor, *W*, that considers several types of energy dissipation. The wave dissipations in the model are due to Darcy flow in porous bottom (Liu & Darlymple, 1984), breaking (when H > 0.78 h) and laminar and turbulent layers (Dean & Darlymple, 1991). In the third case, the Darcy-Weisbach friction factor (*fw*) is used as follows (1):

$$W = \frac{2\omega k\, fw\, |A|\,(1 - i)}{3\pi \sinh 2kh \sinh kh} \quad (1)$$

where *A* is the complex amplitude, *k* is the local wave number, $\omega$ is the wave frequency, and *h* is the depth. The model considers a constant wave factor equal to *fw* = 0.01, regardless of the bottom type.

The formulation has good results for ranges of wave direction of ± 45° in relation to the predominant wave propagation and for the smooth slope bottom (up to 1:3). The model is used to simulate the propagation of a monochromatic wave (period, direction and amplitude) in coastal zones, considering refraction, diffraction, currents, shoaling and energy dissipation due to breaking and bottom friction. Reflection is not considered. There are two types of lateral boundaries: closed and open ones (total reflection). Because it is a parabolic model, it is faster, more efficient and requires less computational memory than others such as those based on elliptical approximation. The dispersion equation used by REF/DIF 1 considers the nonlinear effects by using the Kirby & Darlrymple approximation (1986). The wave-current interaction, based on the Kirby equation (1986), can be considered.

The model employs the finite difference discretization of Crank-Nicolson's implicit method. The wave height, H, the wave direction, θ, the complex amplitude, *A*, and the surface elevation, η, are calculated in each point of the grid.

In this study, the longitudes of the grid of the domain with the related bathymetry range between 55°00 W and 47°10 W and the latitudes, between 35°40 S and 27°10 S. The distances between the points of the grid are 500 m x 500 m, which reproduce adequately the bottom topography in this region. The grids used in REF/DIF 1 have their first grid lines located in the deep water. The size of the grid is calculated respecting the fact that the number of points per wavelength must be above 5 (Kirby & Dalrymple, 1994).

This paper reports the investigation that was carried out in two steps: a) study of refraction and diffraction effects, and b) study of the behavior of the wave propagation due to bottom friction and variations of width and slope in the inner shelf and shoreface.

The refraction-diffraction analysis considers studies about wave climate in RS state (Motta, 1963; Pitombeira, 1975; Strauch, 1988; Coli, 1994, 2000; Fontoura, 2004). According to these studies, predominant waves had the following characteristics: period of T = 9 s, significant height of Hs = 2 m and incident directions equal to 45°, 70°, 90°, 110°, 135°, 160° and 180°.

Regarding the second step, the study of the influence of bottom friction and variations of width and slope in the offshore and the nearshore, two friction factors were used. One refers to the default value of REF/DIF 1 (*fw* = 0.01); the other one was calculated considering the bottom composition. In this case, the bottom is composed by medium sand and gravel and its surface presents wave-ripples, providing high values of *fw* (above 0.30, according to Wright & Short, 1984). Besides, when Martins *et al.* (1999) studied the sand deposits along the inner shelf and shoreface of RS, they identified the presence of bimodal sediments composed by quartz sands and gravel shell fragments from Torres to Mostardas. Indeed, several investigations that applied the side scan sonar have confirmed the existence of sand waves associated to this bottom type. The estimation of *fw* for such bottom, based on Shields' (1936) and Nielsen's (1981) equations and recommendations is approximately 0.2. Therefore, four types of monochromatic waves are simulated without and with bottom friction. The latter uses *fw* = 0.01 and *fw* = 0.2 (Tab. 1). Modal waves (T = 7 s, Hs = 1.75 m and incident directions of 45° and 180°) are typical sea waves which are locally generated by winds, based on Fontoura's investigation (2004). Predominant waves (T = 9 s, Hs = 2 m) are the most frequent ones in the region and have the same directions used in the study of refraction-diffraction. Storm waves (T = 12 s, Hs = 4 m and incident directions of 90°, 135° and 180°) are characterized by Motta (1963). Although rare (occurring at least once per year), these waves correspond to those which reach the shoreline from the south-southeast

with higher energy. Normally, they are associated to high sea level during storms, thus causing important impact and promoting intense erosion processes and strong sediment movement on the coast. Design waves (T = 16 s, Hs = 4.8 m and incident directions of 90°, and 135°) are swell-type waves with low frequency of occurrence (30-year recurrence period), due to extraordinary ocean storms mainly from the southeast.

Table 1. Wave characteristics of the numerical simulations

| Wave characteristics | Direction (*fw* = 0.1) | Direction (*fw* = 0.2) |
|---|---|---|
| Modal (T = 7 s, H = 1.75 m) | 45º and 180º | 180º |
| Predominant (T = 9 s, H = 2.0 m) | 45º, 70º, 90º, 110º, 135º, 160º and 180º | 90º and 135º |
| Storm (T = 12 s, H = 4.0 m) | 90º, 135º and 180º | 135º |
| Design (T = 16 s, H = 4.8 m) | 90º and 135º | 135º |

Three profiles perpendicular to the coast located in Tramandaí, Pinhal and Quintão (Fig. 2) are used to analyze the variation of the wave height along this direction, similar to the procedure adopted by Wright *et al*. (1987). Tramandaí was chosen because it is a region where the bathymetry of 20 m is closer to the coast, which characterizes a narrow shoreface and a wide inner shelf. On the other hand, Quintão is a region where this bathymetry is farther away (wide shoreface and narrow inner shelf) and Pinhal is the region that limit both areas. The bottom slopes in zones with bathymetries between 0 and 20 m (nearshore limits) are 1:549, 1:367 and 1:335, related to Quintão, Tramandaí and Pinhal, respectively. It is possible to notice that Quintão region has a gentler bottom slope (1:549) by comparison with the other ones. In zones where range of bathymetry is 20 m to 50 m (nearshore limits), the slopes are 1:332, 1:348 and 1:334 (Quintão, Tramandaí and Pinhal, respectively). Since the bathymetry is equal to 30 m, the Quintão slope is the highest one (1:332). Between 50 m and 80 m, the Quintão slope (1:572) is still steeper, followed by Pinhal (1:670) and Tramandaí (1:742).

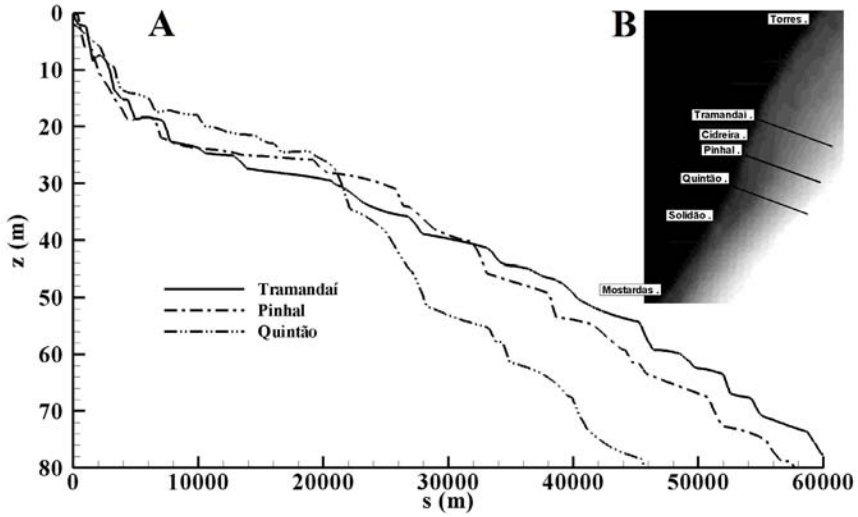


Figure 2. Tramandaí, Pinhal and Quintão profiles (A) and their locations (B).

## 3 Results and discussions

### *3.1 Refraction-diffraction*

The numerical simulations consider deep water boundary conditions for a wave period T=9s and directions 45°, 70°, 90°, 110° 135°, 160° and 180°. The wave rays began changing the directions in $L_o/4$ depth (where $L_o$ is the wavelength in deep water condition), due to the influence of the bottom on the wave dynamics. Figure 3 presents the wave rays for 45º, 90º, 135º and 180º directions. The mean distance between the wave rays is 5.5 km in deep water for all wave incidences. Figure 4 shows, in large scale, the refraction pattern obtained through the numerical simulation. The zones were classified in three groups according to the variation of the distances between wave rays from the deep water to the shoreline. They are divergent (D), in cases in which distances between wave rays increase more than 10 %; convergent (C), for distances between wave rays that decrease more than 10 %; and invariable (I) in cases 10 % variation is not reached. The analysis highlighted that the dominant pattern is divergent and invariable for 90° and 135° almost all over the coast, except in the southern region of Quintão, where divergence occurs.

Speranski & Calliari (2006) studied the wave refraction on RS coast and concluded that relative long waves, with periods of T ≥ 9 s, from northeast-east and south-southeast-southwest, present the divergent pattern, while waves from east-south-southeast have invariable behavior.

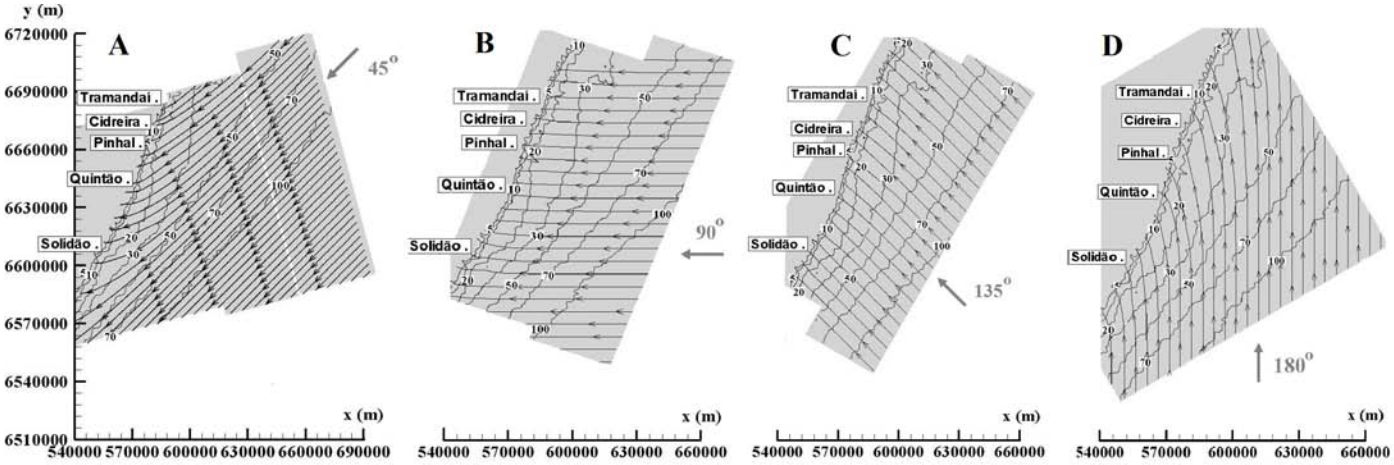


Figure 3. Wave rays for T = 9 s, Hs = 2.0 m, θ = 45° (A), 90° (B), 135° (C) and 180° (D) (Mercator Projection – MC 51°).

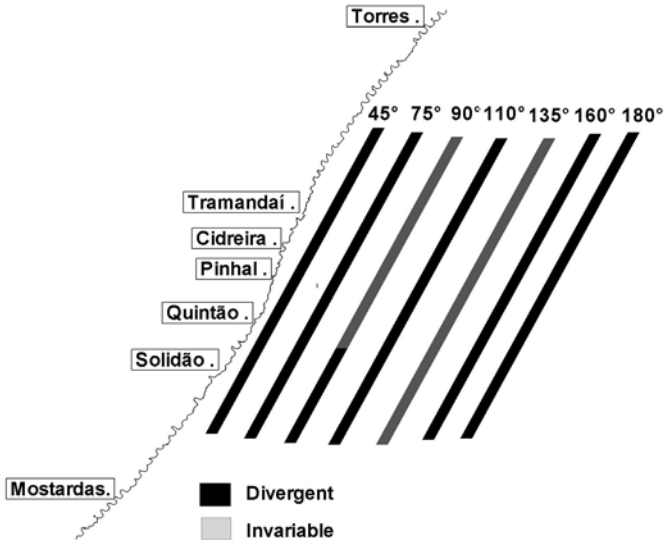


Figure 4. Refraction patterns for waves T = 9 s and Hs = 2 m.

The results that have been reported in this paper are similar to those found by Speranski & Calliari (2006). It is important to emphasize that REF/DIF 1 is based on a more complete formulation than the one applied by these authors. Differences were observed in a shorter-scale length: convergences south of Quintão (110°, 135°, 160° and 180°) and between Cidreira and Pinhal (110° and 135°) for southeast and south waves (Fig. 3). The convergence located south of Quintão is related to the position of Berta shoal which generates a quasi permanent focus close to the breaking zone, as shown in Fig. 5. Such local convergence can be explained by the gentle shoreface and the steep inner shelf found just at the transition between Quintão and the northern adjacent zone, which corroborates with Martinho *et al*.'s findings (2009) regarding the wave convergence and high breaker heights along coastal projections. Other authors (Healy, 1987; Calliari *et al*., 1998; Speranski & Calliari, 2000) demonstrated that the wave ray convergence can be linked to erosion in adjacent coastal zones. Speransky & Calliari (2000) noticed two stable focuses related to erosion areas on the RS coast: one at the Conceição ligthhouse and another on Hermenegildo beach. Esteves *et al*. (2002) reported coastline retraction between Quintão and Solidão whereas Toldo Jr. *et al*. (2006) showed that there is a strong retrogradation of the coastline from Tramandaí to Quintão.

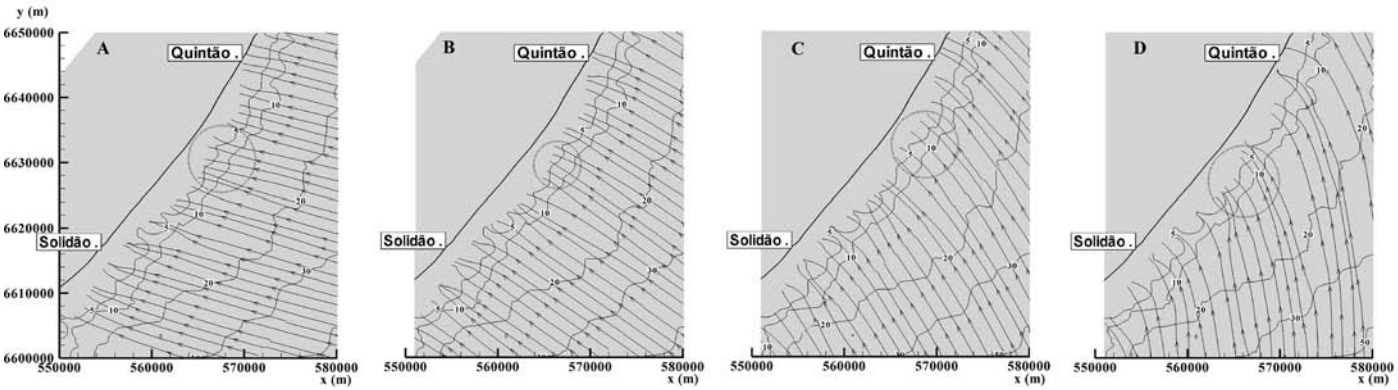


Figure 5. Wave rays close to Solidão and Quintão for T = 9s, Hs = 2.0 m, θ = 110° (A), 135° (B), 160° (C) and 180° (D) (Mercator Projection – MC 51°).

### *3.2 Study of the influence of bottom friction and variations of width and slope on the inner shelf and shoreface*

#### *3.2.1 Friction factor fw = 0.01*

Analyses related to the wave propagations for periods T = 7 s and 9 s indicate that the friction phenomenon practically does not affect the results. Figure 6 represents wave height distributions without and with friction using *fw* = 0.01 for T = 9 s. In waves with these periods, the bottom dynamic is not sufficiently intense to cause significant energy dissipation due to friction. On the other hand, the wave height distribution for T = 12 s (Fig. 7) shows smooth energy attenuation due to bottom friction, with more intensity at the Quintão region. Such result was expected since waves with higher periods provide more intense dynamics on the bottom and, consequently, more frictional dissipation.

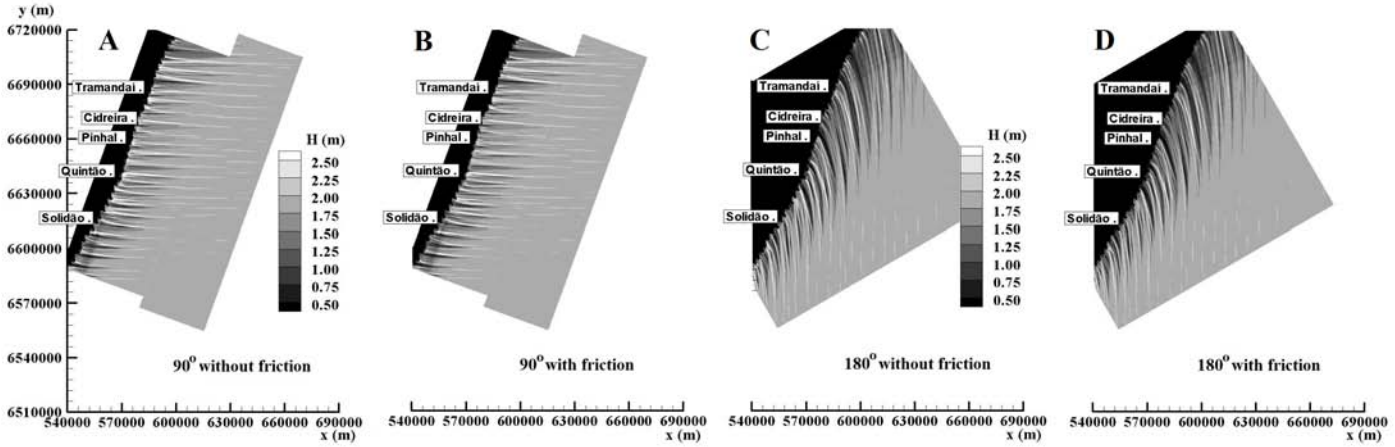


Figure 6. Wave height distribution for T = 9 s, Hs = 2 m, θ = 90° without (A) and with friction (B) and 180° without (C) and with friction (D) (*fw* = 0.01) (Mercator Projection – MC 51°).

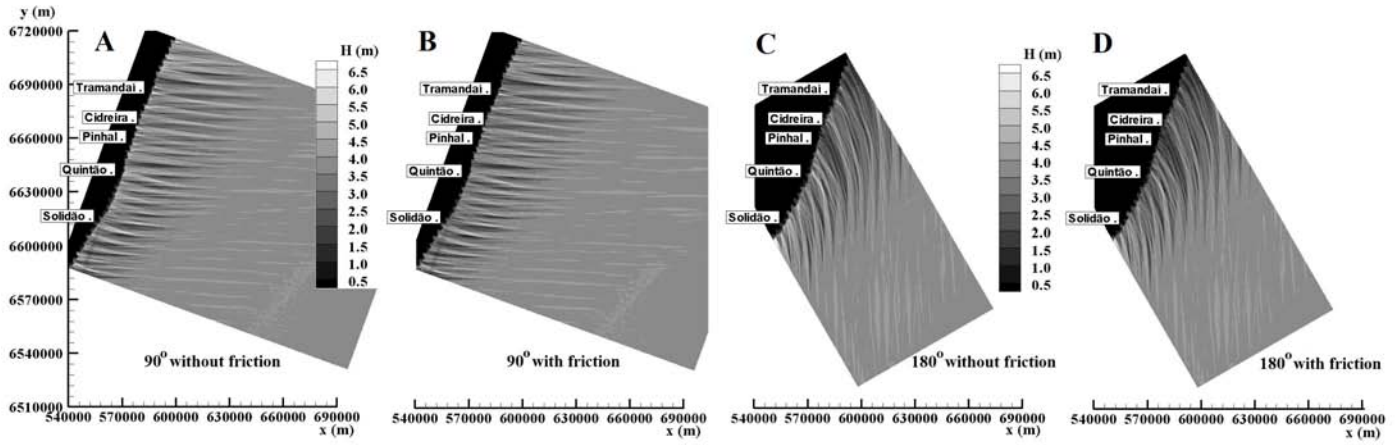


Figure 7. Wave height distribution for T = 12 s, Hs = 4.0 m, θ = 90° without (A) and with friction (B) and 180° without (C) and with friction (D) (*fw* = 0.01) (Mercator Projection – MC 51°).

The wave heights without and with friction along the bathymetries of 20 m and 10 m and their differences (dH) for T = 12 s and incident direction equal to 135° are shown in fig. 8 and 9, respectively. At the 20 m isobaths, the average difference between the wave height without and with friction is dH = 0.23 m, while, at 10 m depth, this difference is dH = 0.48 m. It shows the higher influence of the friction as the waves approach the coast, although these differences keep small (around tenth of meters).

Figure 10 shows the behavior of wave height along the profiles of Tramandaí, Pinhal and Quintão for T = 12 s and incident direction equal to 135°. Significant wave height variations start from 60 m depth for the Tramandaí and Pinhal profiles and from 50 m depth for the Quintão one. The friction influence starts in bathymetries of 51, 53 and 48 m for the Tramandaí, Pinhal and Quintão profiles, respectively. Differences between wave heights without and with friction are more visible from 25 m depth for the Tramandaí and Pinhal profiles and from 15 m for the Quintão one. The highest wave height differences are found up to the wave breaking, when the wave height falls suddenly. These figures confirm that the friction influence is more significant for wave period equal to 12 s by comparison with that related to wave periods of 7 and 9 s, because of the higher wave dynamics on the bottom for 12 s wave periods.

The wave height distributions obtained for design waves (T=16 s) are shown in fig. 11. As expected, by comparison with other periods, differences between without and with bottom friction are more significant in this case.

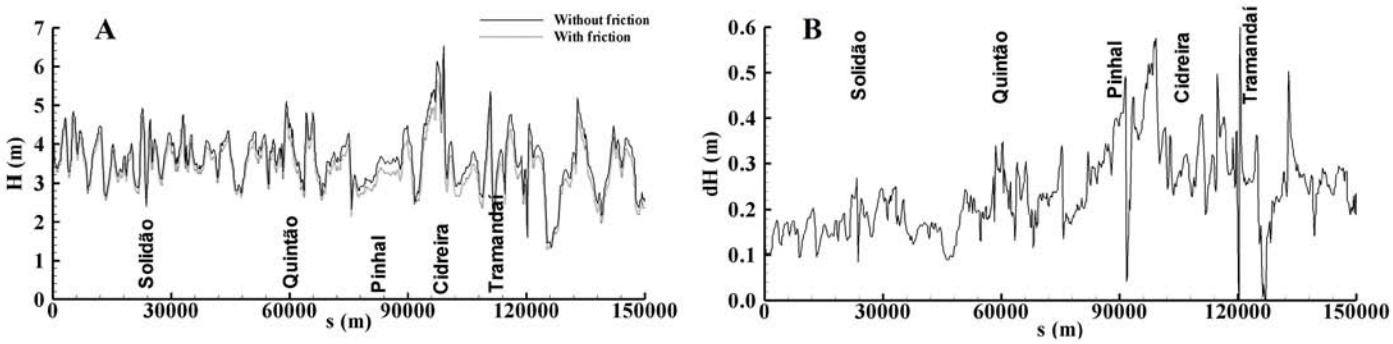


Figure 8. Wave heights (A) and differences between without and with friction (B) along the 20 m isobath for T = 12s, Hs = 4.0m, θ = 135° (*fw* = 0.01).

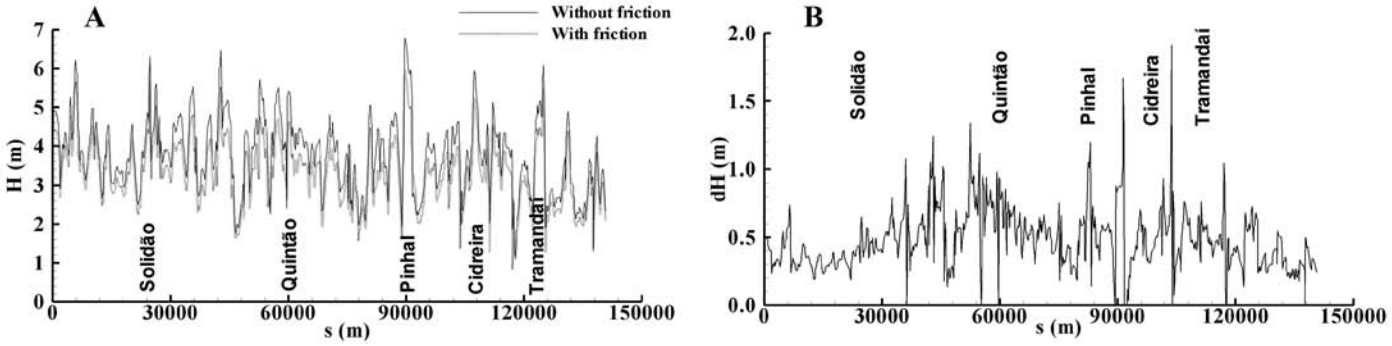


Figure 9. Wave heights (A) and differences between without and with friction (B) along bathymetry of 10 m for T = 12 s, Hs = 4.0 m, θ = 135° (*fw* = 0.01).

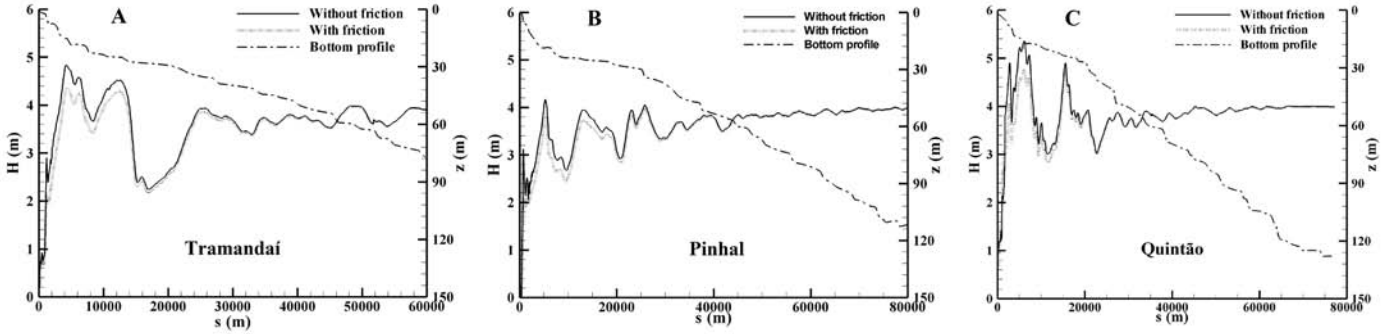


Figure 10. Wave heights for Tramandaí (A), Pinhal (B) and Quintão (C) profiles and T = 12 s, Hs = 4.0 m, θ = 135° (*fw* = 0.01).

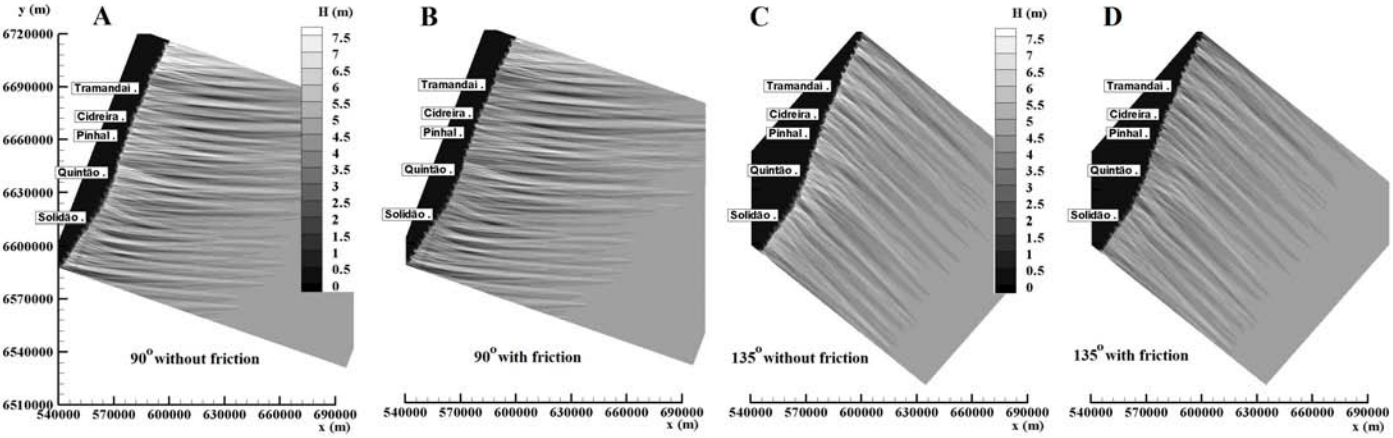


Figure 11. Wave height distributions for T = 16 s, Hs = 4.8 m, θ = 90° without (A) and with friction (B) and 135° without (C) and with friction (D) (*fw* = 0.01) (Mercator Projection – MC 51°).

Figures 12 and 13 show the wave heights and differences between without and with friction along the bathymetries of 20 m and 10 m for design wave. The average differences between wave height without and with friction are dH = 1.07 m and dH = 0.50 m for 10 m and 20 m depths, respectively. Although the nearshore between Quintão and Cidreira is wider, differences in lateral gradients do not occur at the 10 m isobaths (Fig. 13). The differences in average wave heights between without and with bottom friction for waves with T = 16 s (approximately 1.0 m) were larger than those obtained in other periods. The main reason for this fact is that the wave dynamics on the bottom and, consequently, the bottom friction, increases with the wave period.

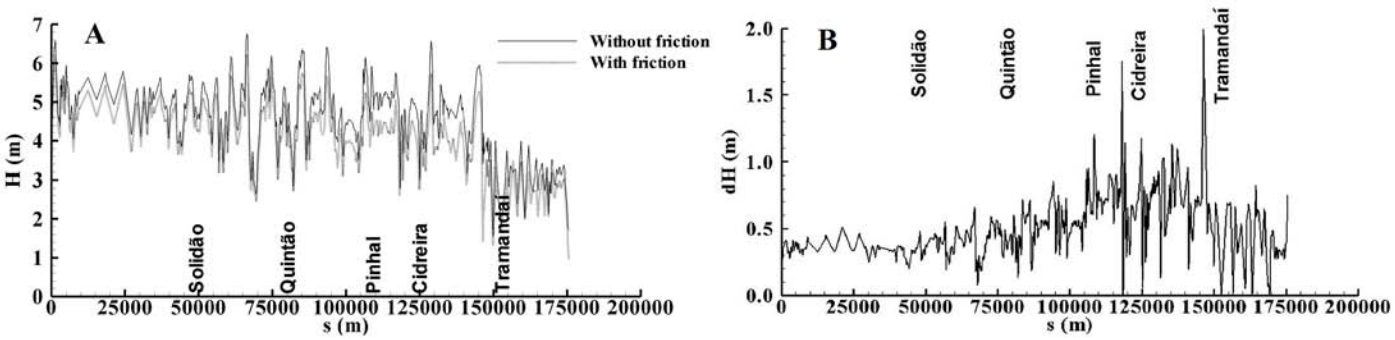


Figure 12. Wave heights (A) and differences between without and with friction (B) for bathymetry of 20 m for T = 16 s, Hs = 4.8 m, θ = 135° (*fw* = 0.01).

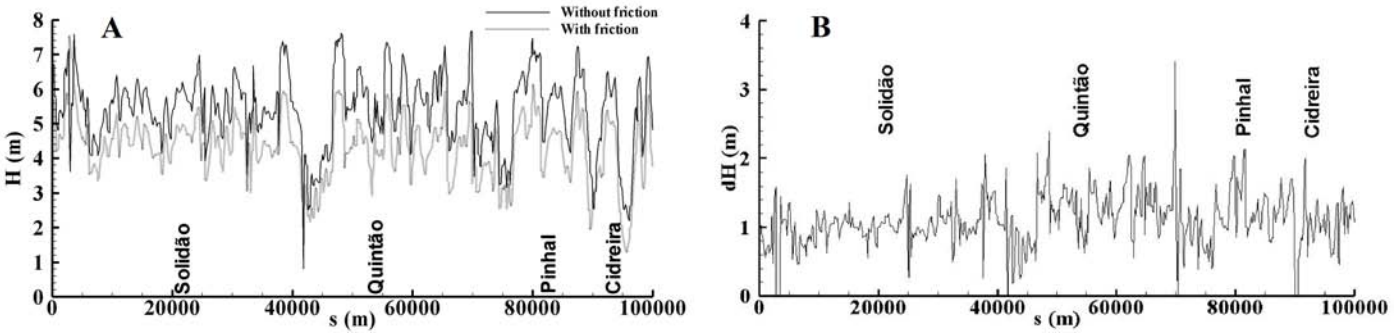


Figure 13. Wave heights (A) and differences between without and with friction (B) for bathymetry of 10 m for T = 16 s, Hs = 4.8 m, θ = 135° (*fw* = 0.01).

The behaviors of the wave heights along the Tramandaí, Pinhal and Quintão profiles (Fig. 14) show that the influence of the friction starts at the bathymetries of 48, 62 and 51 m, respectively. The significant height modifications occur in bathymetries of 135, 105 and 131 m, respectively.

Taking into account the direction, the period and the height combinations, the bottom friction (*fw* = 0.01) does not influence significantly the wave height close to the breaking line, except in the design wave case (T=16 s). The latter presents differences between with and without friction (approximately 1 m at the 10 m isobaths).

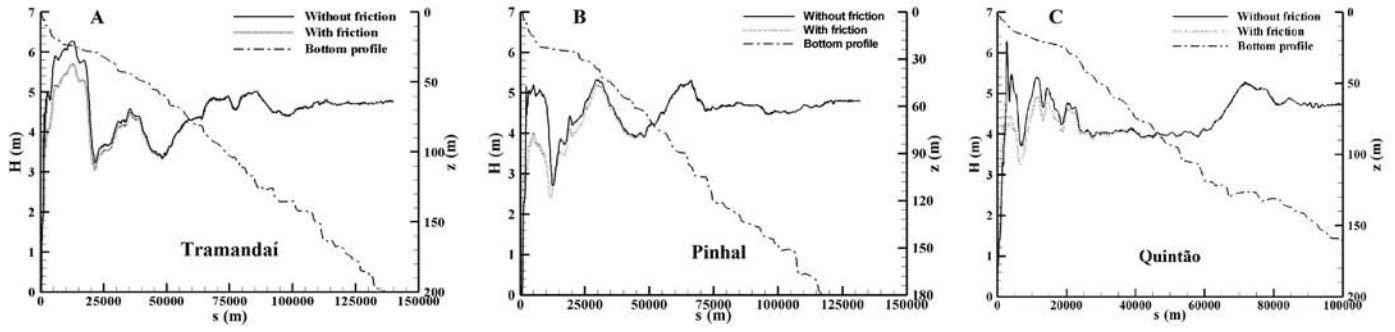


Figure 14. Wave heights for Tramandaí (A), Pinhal (B) and Quintão (C) profiles for T = 16s, Hs = 4.8 m, θ = 135° (*fw* = 0.01).

*3.2.2 Friction factor fw = 0.2*

In all cases, when the friction factor is 0.2, there is strong attenuation as the waves approach the coast, unlike what occurred when using *fw* = 0.01. Figure 15 shows the wave height distribution with and without friction (*fw* = 0.2) for waves T = 9 s and 12 s and θ = 135°.

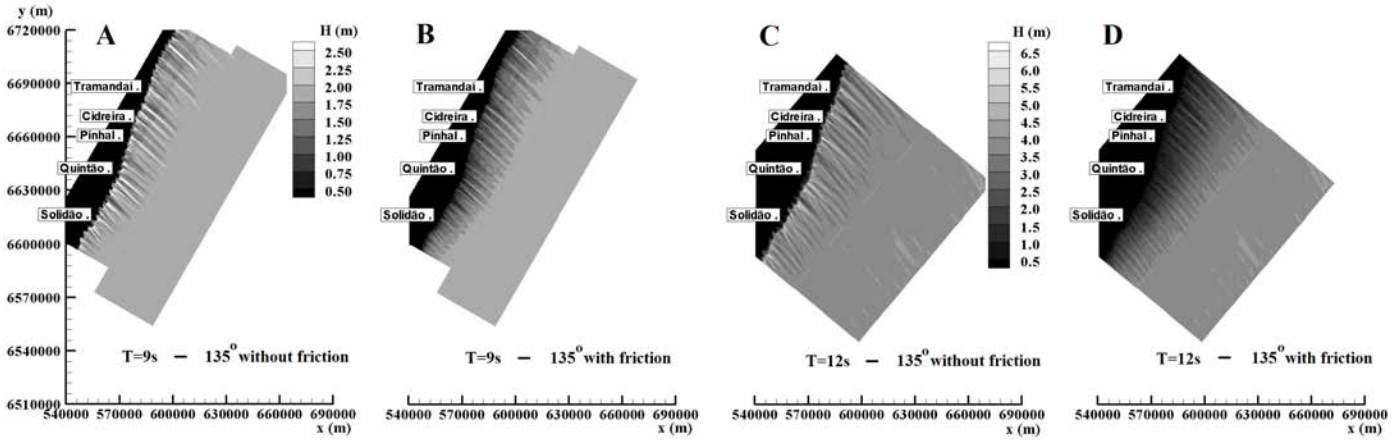


Figure 15. Wave height distributions for θ = 135°, T = 9s without (A) and with friction (B) and T = 12s without (C) and with friction (D) (*fw* = 0.2) (Mercator Projection – MC 51°).

The wave heights along the 20 and 10 m isobaths without and with friction, besides their differences for T = 12 s and θ = 135º, are presented in fig. 16 and 17, respectively. The height differences between without and with friction at 20 m are dH = 1.8 m and dH = 2.3 m in the south and the north of Pinhal, respectively. At the 10 m, the differences are dH = 2.8 m and dH = 2.5 m, respectively. These differences show the strong influence of the bottom friction in the wave energy dissipation using *fw* = 0.2.

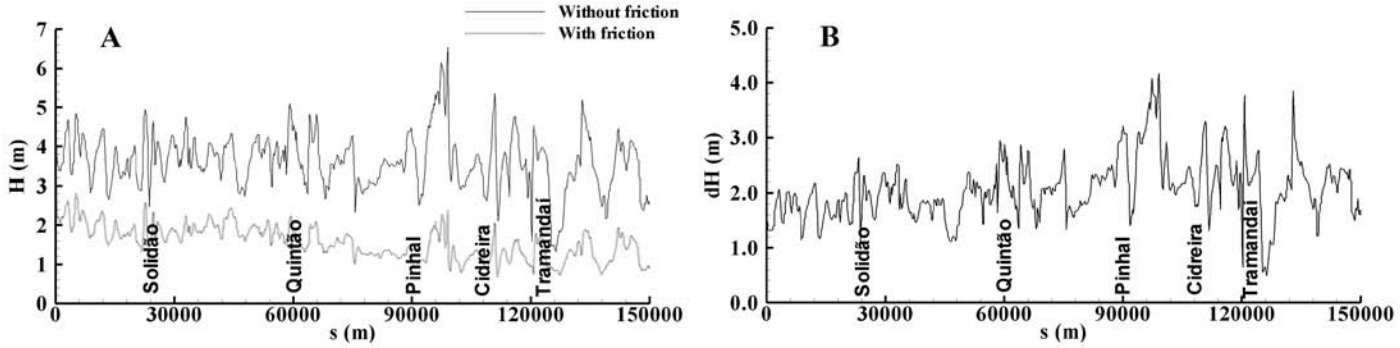


Figure 16. Wave heights (A) and differences between without and with friction (B) along the bathymetry of 20 m for T = 12 s, Hs = 4.0 m, θ = 135° (*fw* = 0.2).

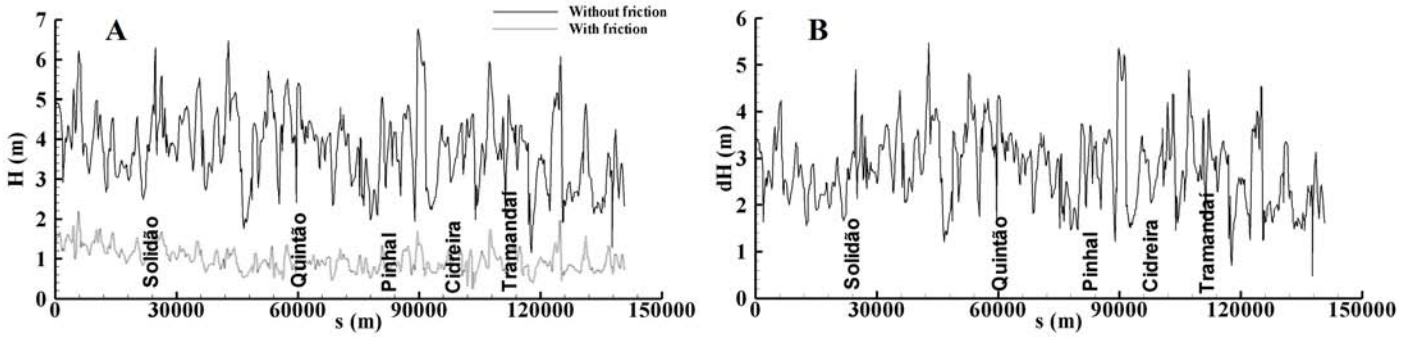


Figure 17. Wave heights (A) and differences between without and with friction (B) along the bathymetry of 10 m for T = 12 s, Hs = 4.0 m, θ = 135° (*fw* = 0.2).

The wave heights along Tramandaí, Pinhal and Quintão profiles for T = 12 s and θ = 135° (Fig. 18) show that the significant wave height variations occur from 68, 60 and 57 m depths, respectively. The influence of the friction starts at 72 m for the Tramandaí and Pinhal profiles and at 68 m for the Quintão one, but it is more intense at 20 m. It can be observed that there is a gradual decrease of the wave height when *fw* = 0.2 is used, i.e., different behavior from *fw* = 0.01 case.

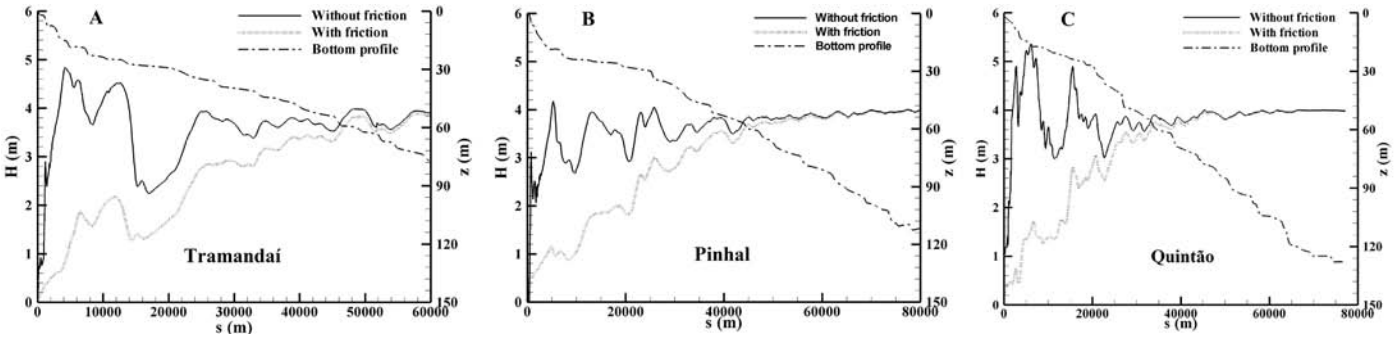


Figure 18. Wave heights along Tramandaí (A), Pinhal (B) and Quintão (C) profiles for T = 12 s, Hs = 4.0 m, θ = 135° (*fw* = 0.2).

The wave height distributions for the design waves (T = 16 s, Hs = 4.8 m and θ = 135°) without and with friction (*fw* = 0.2) are shown in fig. 19. The strong attenuation of the wave is clear, as expected. The behaviors of wave heights along bathymetries of 20 and 10 m are presented in fig. 20 and 21, respectively. Along the bathymetry of 20 m, the average height differences are dH = 3.1 m in the south of Pinhal and dH = 2.9 m in the north of Pinhal, while along the bathymetry of 10 m, these differences are dH = 4.3 m and dH = 4.6 m, respectively.

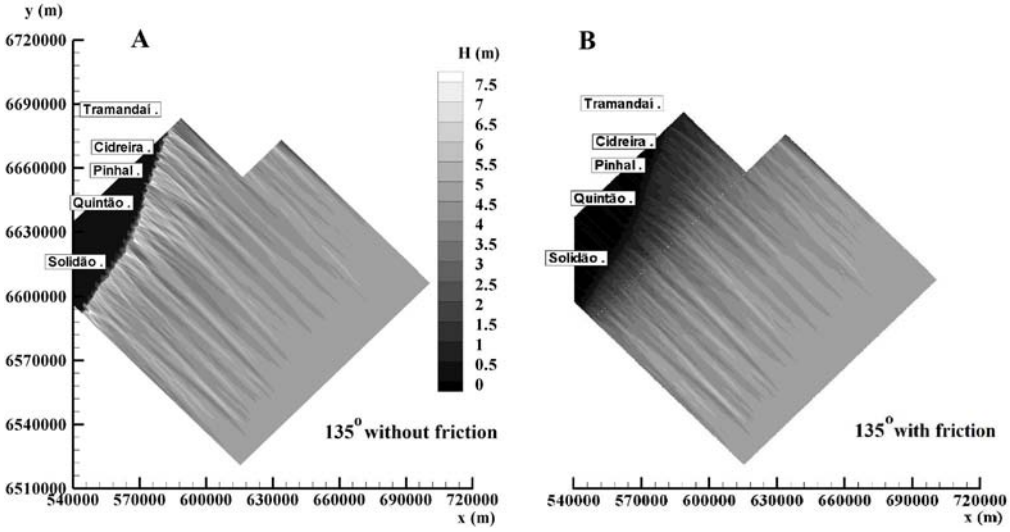


Figure 19. Wave height distributions without (A) and with friction (B) (*fw* = 0.2) for T = 16 s, Hs = 4.8 m, θ = 135° (Mercator Projection – MC 51°).

The wave heights along the Tramandaí, Pinhal and Quintão profiles (Fig. 22) show that the significant wave height variations occur from 112, 117 and 116 m depths, respectively. The influence of the friction starts at 142 m for the Tramandaí and Pinhal profiles and at 150 m for the Quintão one. This influence is more important from 70 m depth for the Tramandaí profile and 50 m for the Pinhal and Quintão ones.

Wrigth *et al.* (1987), in their investigation about the beach dynamics in the coastal region of Virginia state, between Cape Henry and False Cape, observed that there was more energy dissipation due to bottom friction in shallower and smoother slope regions than in deeper and steeper ones. Additionally, the authors noticed that waves reached the coast with higher height in narrow nearshore. Since, in this case, the inner shelf width does not vary along the region, the lateral energy gradient and, consequently, the erosion effects occurred because of the shoreface width variation, as reported by Healy (1987) and Reeve *et al.* (2012) and others.

In contrast to the case studied by Wrigth *et al.* (1987), in the coastal region between Torres and Mostardas, there were no important height differences between narrow and wide nearshore regions along the 10 m isobath when the influence of friction was significant. The reason for this behavior is that the narrow nearshore (20 m depth) has a wide offshore (50 m depth). This characteristic compensates the energy dissipation in comparison with another region that has the inverse situation. From Pinhal

to Tramandaí (where the distance between bathymetries of 50 and 20 m is 38.7 km) the wave heights at the 20 m are lower than those from Solidão to Pinhal (where this distance is 14.86 km), but at the 10 m isobath, the heights are practically similar, showing the compensation of the zone between 20 and 10 m depth.

Table 2 shows the average height differences between without and with friction (*fw*=0.2) and observations for several wave periods and directions. According to these comments, in general, there are compensations of energy dissipation along the inner shelf and shoreface.

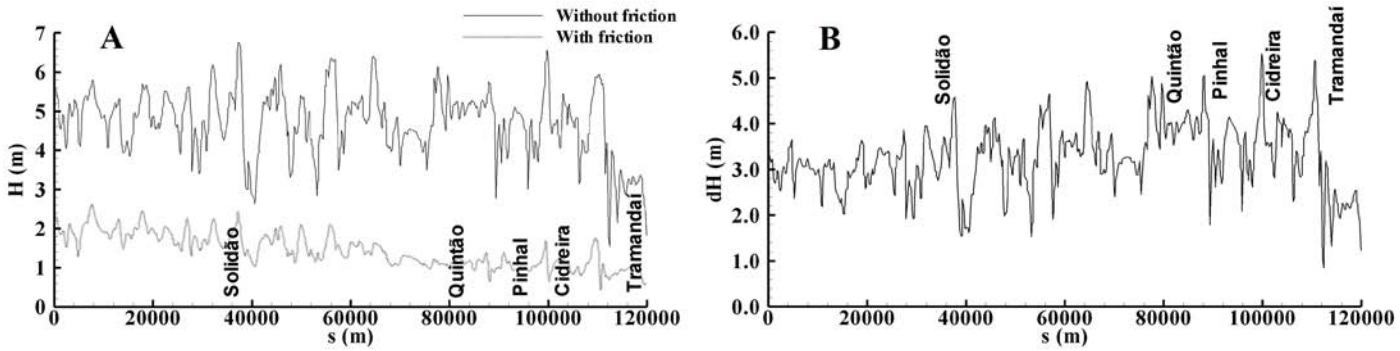


Figure 20. Wave heights (A) and differences between without and with friction (B) (*fw* = 0.2) along the bathymetry of 20 m for T = 16 s, Hs = 4.8 m, θ = 135°.

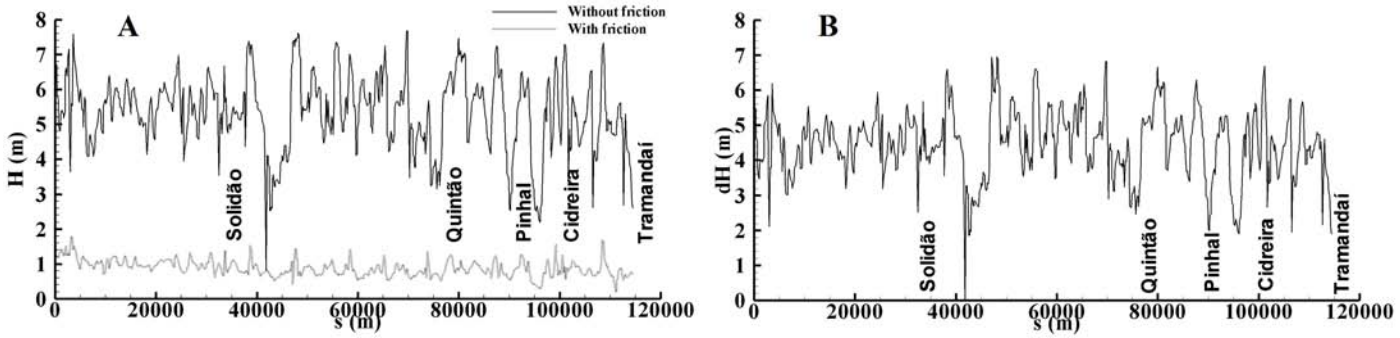


Figure 21. Wave heights (A) and differences between without and with friction (B) (*fw* = 0.2) along the bathymetry of 10 m for T = 16 s, Hs = 4.8 m, θ = 135°.

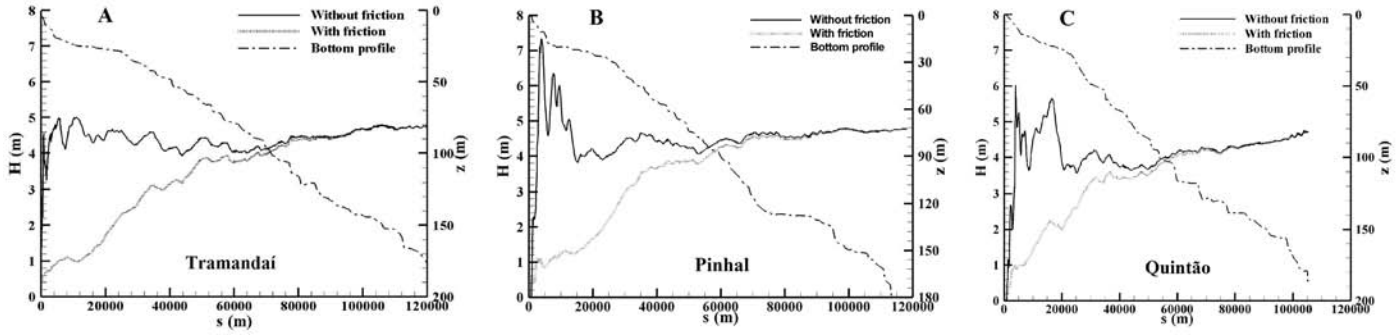


Figure 22. Wave heights along Tramandaí (A), Pinhal (B) and Quintão (C) profiles for T = 16s, Hs = 4.8m, θ = 135° (*fw* = 0.2).

Table 2. Average height differences between without and with friction (*fw* = 0.2). SP = south of Pinhal and NP = North of Pinhal.

| T – θ | dH (m) | | | | Comments |
|---|---|---|---|---|---|
| | z = 20m | | z = 5m or 10m | | |
| | SP | NP | SP | NP | |
| 9s – 90° | 0.4 | 0.5 | 1.2 | 1.4 | Energy compensation. Smooth convergence south of Solidão |
| 9s – 135° | 0.4 | 0.5 | 1.1 | 1.2 | Energy compensation. Little variation, but with a smooth divergence north of Pinhal |
| 7s – 180° | 0.15 | 0.2 | 0.5 | 0.3 | Shoreface influence is slightly higher<br>Little divergence north of Pinhal |
| 12s – 135° | 1.8 | 2.3 | 2.8 | 2.5 | Shoreface influence is slightly higher Little divergence north of Pinhal<br>Little variations |
| 16s – 135° | 3.0 | 3.2 | 4.3 | 4.5 | Inner shelf influence is slightly higher<br>Bottom friction is more important<br>Divergence north of Pinhal |

## 4 Conclusions

A characterization of the main processes of wave propagation by numerical simulation on the central and northern coast of RS, Brazil, specifically between Torres and Mostardas, was presented in this paper. REF/DIF 1, which takes into account all wave transformation processes from deep to shallow waters, was employed. Other studies were also developed in this region; however they used simplified method (reflection, diffraction, friction bottom and current-wave interaction are not considered), based on the numerical scheme of Griswold (1963) (Pimenta, 1999; Speranski & Calliari, 2006). The refraction-diffraction study indicates a dominant divergent pattern. For a 90º wave approach, the pattern remains the same, except for divergence occurring south of Quintão. In short scale, convergence, due to the Berta Shoal, occurs south of Quintão for waves coming from 110°, 135°, 160° and 180°.

In all simulations with the friction factor *fw*=0.01, the wave energy did not decrease significantly. The exception was for the design wave (T = 16 s, Hs = 4.8 m), in which these differences were around 1 m. The inner shelf area from 50 to 20 m depth does not contribute to wave energy dissipation for *fw* = 0.01 and, consequently, there are no significant lateral gradients in wave energy for *fw* = 0.01. There is more energy dissipation using *fw* = 0.2 and the shoreface has important influence in terms of wave dissipation. Attenuation of wave energy increases when waves have higher periods and significant heights using *fw* = 0.2. However, there are no significant lateral gradients for *fw* = 0.2, i.e., the wave heights along the 5 and 10 m isobath have few variations. This study showed the importance of the correct evaluation of the friction factor *fw* to determine the wave energy dissipation due to the bottom friction. The knowledge of the bottom types (sediment and morphology) of the region enables to take into account the space variation of *fw* that provides more accurate results.

**Acknowledgements -** The authors acknowledge the funding of Conselho Nacional de Desenvolvimento Científico e Tecnológico (CNPq).

## References

Calliari, L.J., Speranski, N.S. & Boukareva, I.I. 1998. Stable focus of wave rays as a reason of local erosion at the Southern Brazilian coast. *In*: INTERNATIONAL COASTAL SYMPOSIUM, 1998, Florida. *Anais*... Florida, ICS98, p. 19-23.

Coli, A.B. 1994. *Análise das Alturas de Onda ao Longo do Rio Grande do Sul: Dados Históricos e Altimétricos*. Rio Grande, 58p. Graduation monography, Oceanology Course, Universidade Federal do Rio Grande (FURG).

Coli, A.B. 2000. *Estudo do Clima Ondulatório em Rio Grande*. Rio Grande, 76p. Master's thesis, Post-graduation in Ocean Engineering, Universidade Federal do Rio Grande (FURG).

Dean, R.G. & Darlymple, R.A. 1991. *Water Wave Mechanics for Engineers and Scientists*. Singapore, World Scientific, 353p.

Ebersole, B.A. 1985. Refraction-difraction model for linear water waves. *Journal of Waterways, Port, Coastal, and Ocean Engineering*, 3(6): 939-953.

Esteves, L.S., Toldo Jr., E.E., Dillenburg, S.R. & Tomazelli, L.J. 2002. Long-and short-term coastal erosion in southern Brazil. *Journal of Coastal Research*, 36: 273-282.

Fontoura, J.A.S. 2004. *Hidrodinâmica costeira e quantificação do transporte longitudinal de sedimentos não coesivos na zona de surfe das praias adjacentes aos molhes da Barra do Rio Grande, RS, Brasil*. Porto Alegre, 281p. Doctoral Dissertation, Post-graduation in Hydric Resources and Environmental Sanitation, Instituto de Pesquisas Hidráulicas, Universidade Federal do Rio Grande do Sul.

Griswold, G.M. 1963. Numerical calculation of wave refraction. *Journal of Geophysical Research*, 8(6): 1715-1723.

Healy, T. 1987. The importance of wave focusing in the coastal erosion and sedimentation process. *In*: COASTAL SEDIMENTS'87, New York. *Anais*... New York, ASCE, p.1472–1485.

Kirby, J.T. 1986. Rational approximations in the parabolic equation method for water waves. *Coastal Engineering*, 10: 355-378.

Kirby, J.T. & Dalrymple, R.A. 1986. An approximate model for nonlinear dispersion in monochromatic wave propagation models. *Coastal Engineering*, 9: 545-561.

Kirby, J.T. & Darlymple, R.A. 1994. Combined refraction/Diffraction Model, REF/DIF 1. Version 2.5. Documentation and User's Manual, Center for Applied Coastal Research. Department of Civil Engineering. University of Delaware, Newark 19716.

Liu, P.L.F. 1990. Wave Transformation. *In:* Le Mehaute, B. & Hanes, D.M. (Ed.). *The Sea Ocean Engineering Science*, New York, J. Willey and Sons, 9A, p. 27-63.

Liu, P.L.F. & Darlymple, R.A. 1984. The Damping of Gravity Water Waves Due to Percolation. *Coastal Engineering*, 8: 33-49.

Liu, P.L.F. & Losada, I.J. 2002. Wave propagation modeling in coastal engineering. *Journal of Hidraulic Research*, 40 (3): 229-240.

Martinho, C.T., Dillenburg, S.R. & Hesp, P. 2009. Wave energy and longshore sediment transport gradients controlling Barrier Evolution in Rio Grande do Sul, Brazil. *Journal of Coastal Research*, 25(2): 285-293.

Martins, L.R., Martins, I.R. & Wolff, I.M. 1999. Sand deposits along Rio Grande do Sul, (Brazil) inner continental shelf. *In*: Martins, L.R. and Santana, I. (Ed.). *Non Living Resources of the Southern Brazilian Coastal Zone and Continental Margin*. Porto Alegre, OAS/IOC-UNESCO/MCT, p. 26-38.

Motta, V.F. 1963. *Análise e previsão das alturas de ondas em Tramandaí*. Porto Alegre, Instituto de Pesquisas Hidráulicas, Universidade Federal do Rio Grande do Sul, 30p. (Report).

Nielsen, P. 1981. Dynamics and geometry of wave generated ripples. *Journal of Geophysical Research*, 86(C7): 6467-6472.

Pimenta, F.M. 1999. *Caracterização dos regimes de refração de onda ao longo da zona costeira do Rio Grande do Sul*. Rio Grande, 66p. Graduation monography, Oceanology Course, Universidade Federal do Rio Grande (FURG).

Pitombeira, E.S. 1975. *Estimativa do volume anual de trans-*

*porte litorâneo na costa do Rio Grande do Sul*. Porto Alegre, 96p. Master's thesis, Post-graduation in Hydric Resources and Environmental Sanitation, Instituto de Pesquisas Hidráulicas, Universidade Federal do Rio Grande do Sul.

Reeve, D., Chadwick A. & Fleming, C. 2012*. Coastal Engineering: Processes, Theory and Design Practice*. London. Taylor & Francis Ltd., 552p.

Shields, A. 1936. Application of similarity principles and turbulence research to bed-load movement. *Mitteilungen der Preussischen Versuchsanstalt für Wasserbau und Schiffbau*, 26: 5-24.

Speranski, N. & Calliari, L.J. 2000. Bathymetric lenses and localized coastal erosion in Southern Brazil. *Journal of Coastal Research*, 34: 209-215.

Speransky, N.S. & Calliari, L.J. 2006. Padrões de Refração de Ondas para a Costa do Rio Grande do Sul e sua Relação com a Erosão Costeira. *In*: Muehe D. (Ed.) *Erosão e Progradação do Litoral Brasileiro, RS*. Brasília, Programa de Geologia e Geofísica Marinha, 475p.

Strauch, J.C. 1998. Um ano de monitoramento de ondas em Rio Grande. *In*: XI SEMANA NACIONAL DE OCEANOGRAFIA, Rio Grande. *Anais*... Rio Grande, FURG, p. 1-10.

Toldo Jr., E.E., Almeida, L.E.S.B., Nicolodi, J.L. & Martins, L.R. 2006. Erosão e Acresção da Zona Costeira. *In*: Muehe D. (Ed.) *Erosão e Progradação do Litoral Brasileiro, RS*. Brasília, Programa de Geologia e Geofísica Marinha, 468-474.

Wright, L.D. & Short, A.D. 1984. Morphodynamic variability of surf zones and beaches: A synthesis. *Marine geology*, 56: 93-118.

Wright, L.D., Kim, C.S., Hardaway, C.S., Kimball, S.M. & Green, M.O. 1987. *Shoreface and Beach Dynamics of the Coastal Region From Cape Henry to False Cape, Virginia*., Virginia Institute of Marine Science School of Marine Science College of William and Mary Gloucester Point, 115p. (Technical report).

Manuscrito 533.
Editores: Iran S. Correa & Maria do Carmo Lima e Cunha.